Available online at www.sciencedirect.com
SCIENCE DIRECT®
Journal of Nuclear Materials 319 (2003) 59–64
journal of nuclear materials
www.elsevier.com/locate/jnucmat

Zirconate pyrochlore as a transmutation target: thermal behaviour and radiation resistance against fission fragment impact

S. Lutique, D. Staicu, R.J.M. Konings, V.V. Rondinella, J. Somers, T. Wiss *

European Commission, Joint Research Centre, Institute for Transuranium Elements, P.O. Box 2340, D-76125 Karlsruhe, Germany

Abstract

Zirconates with the pyrochlore structure ($A_2Zr_2O_7$) are investigated at ITU for use as an actinide host in inert matrix fuels for transmutation. Zirconate pyrochlores with A = Nd as an inactive stand in for the trivalent actinides Am and Cm were fabricated and characterised, and their thermal transport properties measured. The low thermal conductivity indicates that zirconate pyrochlore can only be used for transmutation if it is dispersed in a cercer or cermet composite fuel. The temperature profiles of a $MgO–An_2Zr_2O_7$ composite were calculated using the measured Nd-zirconate thermal conductivity for different concentrations of the included phase. The radiation stability of $Nd_2Zr_2O_7$ against fission products (FP) was investigated using iodine irradiation (120 MeV). Significant alterations of the implanted regions were observed even at relatively low fluence.

1. Introduction

Aiming at reducing the radiotoxicity of nuclear waste, transmutation of the longest living radionuclides is an innovative option. In this way, minor actinides (e.g. ^{237}Np, ^{241}Am, ^{244}Cm) and/or long lived FP (e.g. ^{129}I, ^{99}Tc) are 'burned' in nuclear reactors by successive neutron captures and/or fission. As these problematic radionuclides are mostly produced by successive neutron captures by ^{238}U in the UO_2 matrix, the substitution of UO_2 by an inert matrix fuel (IMF) or target concept was proposed. Thus UO_2 would be replaced by another compound constituted of elements with low neutron capture cross sections, the so-called *inert matrix*. Several compounds are envisaged, including oxides (e.g.: MgO or ZrO_2), nitrides (e.g.: ZrN) or composites (cercer or cermet). The properties relevant for their use are various [1], and include thermal conductivity not much lower than that for UO_2 and radiation resistance against FP.

Several pyrochlore compounds were extensively studied for nuclear applications (mainly as storage matrices, [2–9]). From the point of view of radiation damage stability and leaching behaviour it appeared that zirconate pyrochlores were more suitable compounds to host radioactive elements compared to titanate pyrochlores. In view of these observations, the use of zirconate pyrochlore as a transmutation target was previously suggested [10,11]. In this context, a study was initiated at ITU concerning pyrochlore zirconates with the general formula $A_2Zr_2O_7$, where A could be either a lanthanide, an actinide, or a combination thereof. The initial investigations were focused on the inactive compound $Nd_2Zr_2O_7$, where Nd is a stand in for the trivalent actinides Am and Cm. The experimentally derived value of thermal conductivity of $Nd_2Zr_2O_7$ was 1.33 $W\,m^{-1}\,K^{-1}$ [12,13]. This value is quite low compared to UO_2 or even to that of stabilised zirconia. Thus, a cercer composite concept must be envisaged to compensate and reduce the operating temperature of the targets for a given actinide

* Corresponding author. Tel.: +49-7247 951 447; fax: +49-7247 951 199.
E-mail address: wiss@itu.fzk.de (T. Wiss).

0022-3115/03/$ - see front matter © 2003 Elsevier Science B.V. All rights reserved.
doi:10.1016/S0022-3115(03)00134-X

loading. A preliminary study of the in-pile temperature profile of a MgO–$Am_2Zr_2O_7$ target with different volume ratios magnesia–pyrochlore was also performed [12]. The results reported there were promising. The present paper extends the previous study and provides a more complete simulation of the in-pile temperature profile for the same composite system by taking account of the distribution of the inclusions and their size.

In addition, during the irradiation process, an IMF or target will experience high damage levels due to the different damaging sources: neutrons, fission fragments (FF), alpha particles and recoil atoms. It should be even considered that the decaying actinides will start to produce α-damage from the moment they will be incorporated in the fuel or target. Alpha particles (5–6 MeV) and their corresponding recoil atoms (~100 keV) will induce displacements in the target lattice (~1700 displacements per decay).

When the irradiation starts, the expected high neutron fluxes will induce displacements of target atoms through elastic collisions. However, the highest damage that will be experienced by the target (or the inclusions in case of a cercer [14]) will arise from the actinide fission events. Each fission (~200 MeV) will produce a spike causing about 100 000 displacements from elastic collisions along the pathway of the two FF. In addition, a highly ionised core where inelastic collisions on target electrons occur could induce additional displacements and local high temperatures (thermal spike). The latter can result in drastic material modification (e.g. amorphisation).

To assess the feasibility of using a pyrochlore as IMF or target (as inclusion in cermet or cercer), its stability against the radiations produced in reactor must also be investigated. The present paper reports preliminary results concerning the behaviour of the neodymium zirconate against FP impact which has been simulated by iodine implantation using an accelerated beam.

2. Experimental methods

2.1. Thermophysical properties calculations

In a previous paper [12], in-pile temperature distributions inside a pellet were calculated for a magnesia–pyrochlore cercer composite target designed for a fast reactor application (pellet diameter 5.2 mm) with a linear power of 250 $W\,cm^{-1}$ and a coolant temperature of 750 K. Simulations were made for different volume fractions (V_D) of pyrochlore using an effective thermal conductivity of the cercer κ_{eff}, calculated according to the equation proposed by Miller [15]:

$$\kappa_{eff} = \kappa_D + (1 - V_D)(\kappa_M - \kappa_D)\left(\frac{\kappa_{eff}}{\kappa_M}\right)^{1/3},$$

where V_D is the volume fraction of the dispersed phase, and κ_D and κ_M the thermal conductivities of the dispersed phase and the matrix, respectively.

Here, the model is improved to take into account of the size and spatial distribution of the pyrochlore inclusions and to consider the effect of a damaged area of 10 μm around the inclusions. A medium constituted by an MgO matrix containing a random distribution of spherical 150 μm diameter pyrochlore inclusions was constructed. This size was chosen as it limits the volumetric fraction of matrix damaged by radiation, based on the considerations of Chauvin et al. [14]. The mathematical model corresponding to this microstructure is a boolean scheme of spheres, their overlapping being allowed. Two dimensional temperature fields were calculated by the finite elements method using the CASTEM 2000 code [16]. The central temperatures corresponding to 3D heat transfer were calculated using the 3D/2D-conductivities ratio, deduced from the ratio of the effective conductivities of composites containing spherical (3D, Maxwell [17]) and cylindrical (2D, Rayleigh [18]) inclusions.

2.2. Fission fragment irradiation

Implantation of iodine ions (120 MeV) was performed at the VIVITRON accelerator (TANDEM type) of the IReS institute in Strasbourg. Pellets with 97% of the theoretical density (TD = 6325 $kg\,m^{-3}$) and with the pyrochlore structure (lattice parameter $a = 1.070 \pm 0.001$ nm, slightly higher than literature data [19]) were used to prepare bulk slices and thin foils for transmission electron microscopy (TEM) investigations. The pellet production method was based on a sol-gel procedure and is described in detail elsewhere [12]. Slices of 1 and 2 mm height and 5.5 mm diameter were cut from the pellets and subsequently polished down to 0.25 μm with diamond paste, and finally annealed at 1473 K for 2 h in air.

The TEM specimens (thin foils) were prepared as followed: disks of 3 mm diameter were cut from slices with a thickness of 250 μm and prethinned by dimpling. Following irradiation they were etched with a 6 keV Ar-ions beam with an incident angle of 6°. A final thinning was performed with decreasing ion current and applied tension to prevent formation of defects on the surface. Two slices were irradiated at ion fluences of 10^{14} and 3×10^{14} cm^{-2} and two prethinned TEM specimens at an ion fluence of 5.6×10^{10} cm^{-2}.

SRIM code [20] calculations were performed to determine the range of the iodine ions in the pyrochlore target as well as the electronic energy loss (dE/dx) and the displacement profile. After irradiation the specimens were analysed by scanning electron microscopy (SEM), TEM (after final thinning) and by X-ray diffraction.

3. Results and discussion

3.1. In-pile temperature field of a cercer composite

Fig. 1 shows typical results obtained for the temperature field in a magnesia–pyrochlore pellet (diameter, $d = 5.2$ mm) with a volume fraction $V_D = 0.3$ of pyrochlore inclusions of 150 μm diameter; the linear power was set at 250 W cm^{-1}. The average temperature field is similar to typical fields obtained for a conventional fuel, but local fluctuations can be observed because of the presence of inclusions and of agglomerates. It is interesting to note how, for the configuration illustrated in Fig. 1 (namely, with the inclusion size chosen), the highest temperature regions are not located at the centre of the inclusions, but rather at the pellet centre. This proves the effectiveness of a hybrid concept in maintaining the maximum temperatures within operational acceptable margins. The highest temperature value reached in the pellet was studied as a function of the volume fraction of pyrochlore in the composite, V_D. Both 2D and 3D calculation results are shown in Fig. 2. The 2D calculated values are slightly higher than those for 3D calculations. As V_D increases, the central temperature increases from 1166 K (value that would be obtained for a thermal conductivity corresponding to pure MgO) to 2437 K (value for a pure pyrochlore pellet).

In order to determine the influence of the distribution of the inclusions, simulations were made using a large number of random distributions for a given volume fraction. The 3D central temperatures obtained for

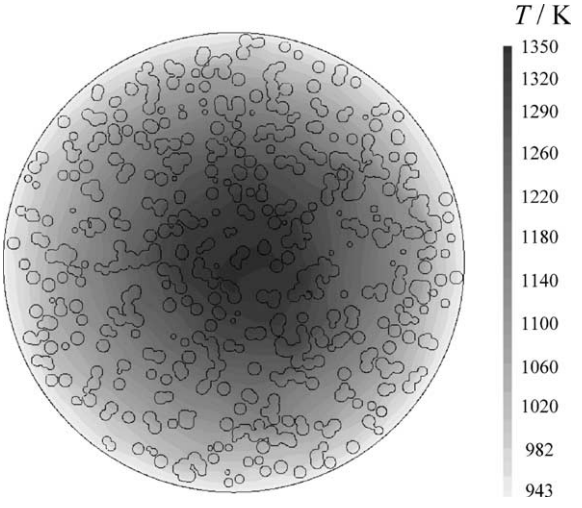

Fig. 1. Typical temperature field obtained from calculation for magnesia–pyrochlore cercer composite (here with $V_D = 0.3$). Calculations were made for fast reactors conditions with a linear power of 250 W cm^{-1}. Pellet diameter of 5.2 mm was taken along with a coolant temperature of 750 K.

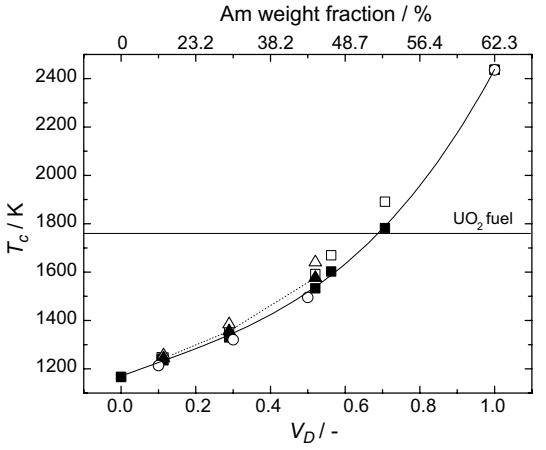

Fig. 2. Central temperature T_c vs. volume fraction of pyrochlore V_D obtained from 2D calculation with or without radiation damage consideration (open triangles and squares) and 3D correction with or without radiation damage consideration (closed triangles and squares) compared with calculated values from effective thermal conductivity corresponding to an equivalent homogeneous solid (open circle, [12]) and conventional UO_2 fuel (solid line).

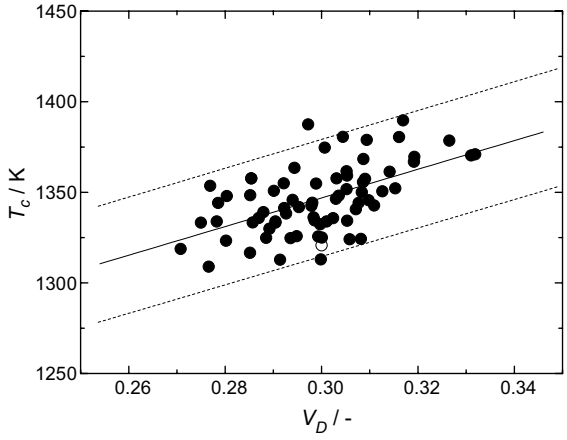

Fig. 3. 3D-central temperature T_c obtained for various random distributions of inclusions with $V_D \sim 0.3$. The open circle corresponds to the homogeneous solid case [12]. The dotted lines represent a ±32 K fluctuation around the linear fitting of the central temperature values.

$V_D \sim 0.3$ are summarised in Fig. 3. The stochastic fluctuation is ~32 K around the central value, which corresponds to ~2.3%. The previous calculations performed using the effective conductivity of the homogeneous solid equivalent to the composite [12] are less than 2% lower than the 3D calculation values (Figs. 2 and 3). For $V_D \sim 0.3$ (Fig. 3), this value falls within the

statistic fluctuations almost at the lowest limit of the range of the central temperature. This is coherent with the fact that such calculation does not take into account of the inclusions size or distribution. These observations confirm the validity of the effective thermal conductivity model that we used in our previous work [12].

The central temperature for a UO_2 fuel with the same linear power is also shown in Fig. 2. This temperature (1760 K) is achieved in the cercer composite for $V_D \sim 0.7$, and is significantly below the melting point or stability limit temperature of each component (i.e. ~2600 K for zirconate pyrochlore [21], 3250 K for MgO [22]). However, it is currently unknown if the system magnesia–pyrochlore presents any eutectic points, with correspondingly lower melting temperature. For safer reactor operation, a temperature margin similar to that for UO_2 should be considered, i.e. 1350 K ($T_M(UO_2) = 3110$ K [22]). This would correspond to a maximum central temperature of 1250 K, which is achieved for $V_D \sim 0.15$, i.e. 18.4 wt% of Am.

Using the same procedure, the temperature field was calculated for the composite including a damaged MgO shell of 10 μm around each inclusion. In this region, 50% of the thermal conductivity of MgO was assumed based on observations done on $MgAl_2O_4$ irradiated in reactor [23]. The influence of such damage on the central temperature value is an increase of approximately 1% for $V_D = 0.1$, 2% for $V_D = 0.3$ and 3% for $V_D = 0.5$.

3.2. Resistance to fission fragment impacts

In order to simulate the damaging effect of FF, samples have been irradiated with a typical FF (iodine) with an energy close to the fission energy (120 MeV) at room temperature. The results of SRIM code calculation in Fig. 4 show the range and the energy losses in the material. The maximum dE/dx value of 22 keV nm^{-1} corresponds to a typical light FP.

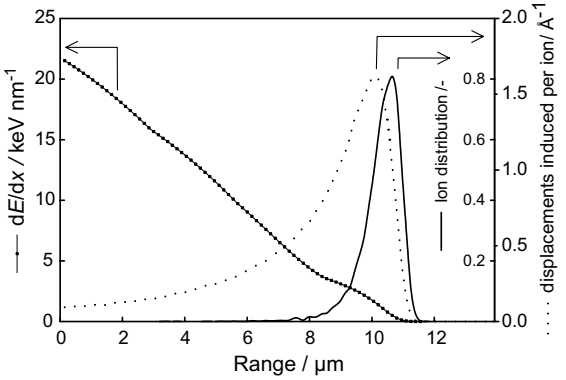

Fig. 4. Range, energy loss and displacement profile of iodine-irradiated $Nd_2Zr_2O_7$, calculated using SRIM2000.

The SEM observations of samples irradiated to ion doses of 10^{14} and 3.0×10^{14} cm^{-2}, shown in Fig. 5(b) and (c), reveal a smoothening of the surface if compared to the unirradiated surface (Fig. 5(a)). No major difference was observed as a function of the fluences. Matter transport occurred in the specimens as a results of ion irradiation: pores and polishing tracks were filled with material as is shown in Fig. 6, where part of the speci-

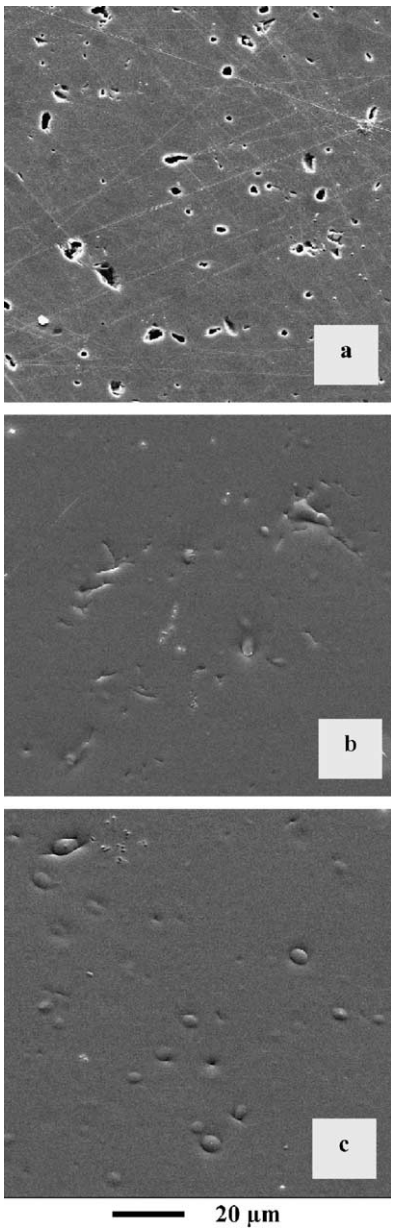

Fig. 5. SEM micrographs of $Nd_2Zr_2O_7$: (a) unirradiated surface, (b) surface irradiated at an iodine ion dose of 10^{14} cm^{-2}, (c) surface irradiated at an iodine dose of 3×10^{14} cm^{-2}.

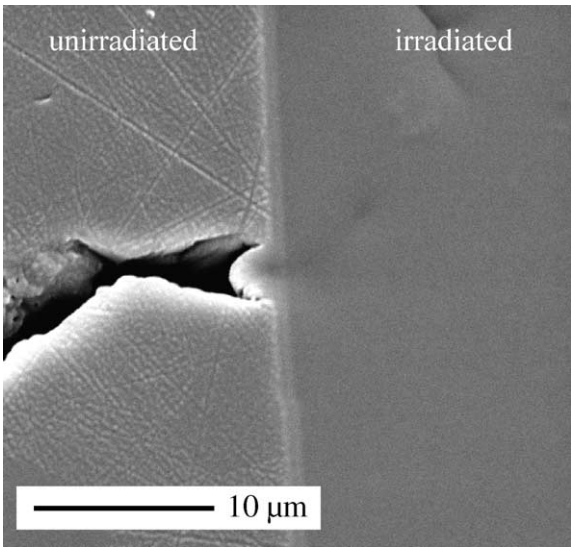

Fig. 6. SEM micrograph of a partly covered sample irradiated at an ion fluence of 3×10^{14} cm^{-2}.

men was covered with a silicon wafer during irradiation at the highest fluence. The disappearance of the polishing tracks can be clearly seen. Additionally, the picture shows complete filling of a pore in the irradiated part. However, profilometry measurements did not however indicate a significant swelling of the irradiated part (no step could be measured between the irradiated/unirradiated areas). XRD analysis of the sample irradiated at a higher fluence revealed the formation of a second crystalline phase. Due to the geometry of the implanted area (half of the pellet), the XRD analysis required to mask the non-irradiated area (a lead foil was used). As a consequence, strong Pb reflections appeared on the XRD pattern but nevertheless allowed the observation of small peaks. This new phase could not be identified as being either ZrO_2(c), ZrO_2(t), ZrO_2(m), Nd_2O_3, $Nd_2Zr_2O_7$ (pyrochlore or fluorite).

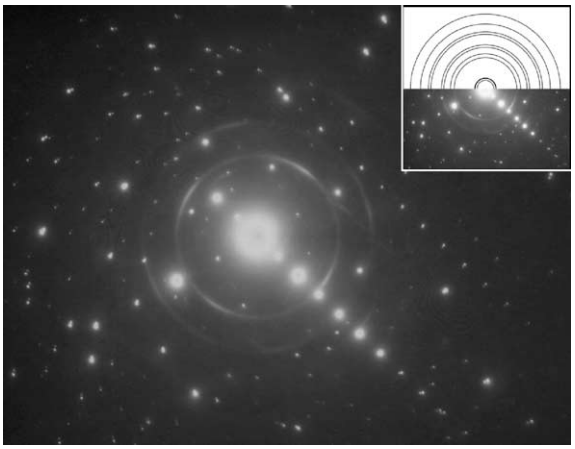

Fig. 8. Electron diffraction pattern of the low fluence irradiated TEM specimen. The upper right inset shows the same diffraction with the corresponding half-circles as determined by the process-diffraction software [26].

TEM observations on samples irradiated at low ion fluence (5.6×10^{10} cm^{-2}) clearly showed evidence for track formation in the pyrochlore. Fig. 7 shows two TEM micrographs exhibiting tracks under normal incident beam condition (a) and with the sample tilted under the electron beam (b). The diameter of the tracks is about 10 nm. This size is large compared to observations made in e.g. $MgAl_2O_4$ where tracks of 6 nm were observed for similar experimental conditions [24]. It has been shown that when the overlap of tracks occurs the material can be rendered amorphous even if the individual tracks are not. Indeed, electron diffraction of the low dose irradiated pyrochlore indicates that a new crystalline phase was formed in the tracks. Concentric rings were observed in the diffraction pattern (see Fig. 8) but the corresponding calculated lattice spacing could not be assigned to any known Zr- and/or Nd-containing phases.

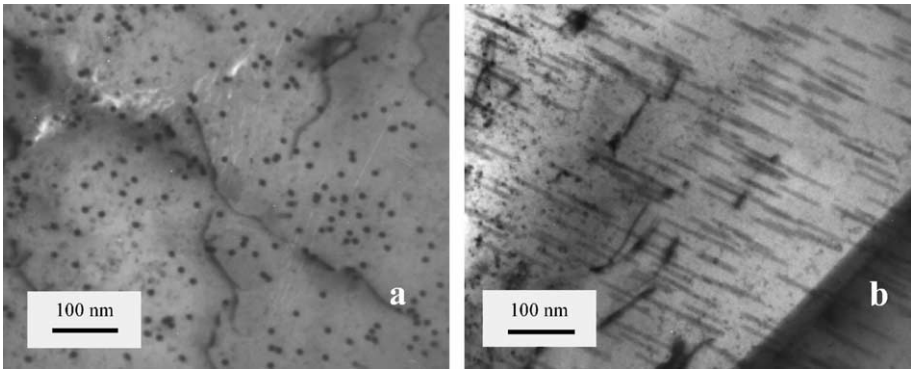

Fig. 7. TEM micrograph of a sample irradiated at an ion fluence of 5.6×10^{10} cm^{-2}: (a) normal incident electron beam condition (b) sample tilted under the electron beam.

4. Conclusion

Given the poor thermal transport properties of Nd-zirconate, a composite concept was considered for use of this material as host matrix for minor actinides transmutation [12]. The in-pile temperature profile of a composite MgO–$Am_2Zr_2O_7$ target with 150 μm inclusions was calculated for fast reactor irradiation conditions. By comparing several random distributions of the inclusions for an almost constant volume fraction ($V_D = 0.3$), a fluctuation of ~60 K was observed for the maximum temperature in the pellet. The central temperature of a conventional UO_2 fuel is achieved for a volume fraction of 0.7 of pyrochlore, which corresponds to a high Am content (~53 wt%). However, respecting the same temperature margin as for a UO_2 fuel, a volume fraction of 0.15 (~18 wt% Am) should be considered as the safe limit for reactor operation of a magnesia–pyrochlore composite. A radiation damage shell of 10 μm in the matrix around the inclusions increases the central temperature less than 3%. Based on these observations, from the point of view of thermophysical properties, pyrochlore zirconate could be used for IMF or target applications as inclusions in a cercer composite.

To assess the damage response against FF, $Nd_2Zr_2O_7$ pyrochlore specimens were irradiated with iodine ions with 120 MeV energy. Matter transport effects and track formation were observed by SEM and TEM, respectively. XRD and electron diffraction patterns indicate the formation of a new crystalline phase. However, irradiation-induced amorphization, which was observed in Ti-based pyrochlores [9], was not observed in $Nd_2Zr_2O_7$ under the irradiation conditions of the present study. Further investigations (e.g. grazing incidence XRD) are necessary to identify the newly formed structure. Based on these findings, the radiation resistance of $Nd_2Zr_2O_7$ against heavy ions with fission energy is not as good as stabilised zirconia [25]. This latter aspect will be further investigated to predict the behaviour of pyrochlore-type zirconate under severe irradiation conditions and assess its applicability for IMF or target configurations.

Acknowledgements

We gratefully thank Dr F. Haas and the team at the Vivitron accelerator, Strasbourg, for the ion irradiations and Mr H. Thiele for the electron microscopy examinations.

References

[1] M. Burghartz, H. Matzke, C. Léger, G. Vambenepe, M. Rome, J. Alloys Compd. 271–273 (1998) 544.
[2] I. Hayakawa, H. Kamizono, Mater. Res. Soc. Symp. Proc. 257 (1992) 257.
[3] I. Hayakawa, H. Kamizono, J. Nucl. Mater. 202 (1993) 163.
[4] S.S. Shoup, C.E. Bamberger, T.J. Haverlock, J.R. Peterson, J. Nucl. Mater. 240 (1997) 112.
[5] K.L. Smith, N.J. Zaluzec, G.R. Lumpkin, J. Nucl. Mater. 250 (1997) 36.
[6] W.J. Weber, J.M. Wald, H. Matzke, Mater. Lett. 3 (1985) 173.
[7] W.J. Weber, J.M. Wald, H. Matzke, J. Nucl. Mater. 138 (1986) 196.
[8] S.X. Wang, B.D. Begg, L.M. Wang, R.C. Ewing, W.J. Weber, K.V. Godivan Kutty, J. Mater. Res. 14 (1999) 4470.
[9] B.D. Begg, N.J. Hess, D.E. McCready, S. Thevuthasan, W.J. Weber, J. Nucl. Mater. 289 (2001) 188.
[10] P.E. Raison, R.G. Haire, Prog. Nucl. Energy 38 (2001) 251.
[11] P.E. Raison, R.G. Haire, in: GLOBAL'01, Paris, 9–13 September 2001.
[12] S. Lutique, R.J.M. Konings, V.V. Rondinella, J. Somers, T. Wiss, J. Alloys Compd. 352 (2003) 1.
[13] S. Lutique, R.J.M. Konings, V.V. Rondinella, J. Somers, T. Wiss, in: CIMTEC 2002, Florence, Italy, 15–18 July 2002.
[14] N. Chauvin, R.J.M. Konings, H. Matzke, J. Nucl. Mater. 274 (1999) 105.
[15] J.V. Miller, Report NASA-TN-D-3898, 1967.
[16] CASTEM 2000, Commissariat à l'Energie Atomique CEA, DRN/DMT/SEMT, 2000.
[17] J.C. Maxwell, A Treatise on Electricity and Magnetism, 2nd ed., Dover, New York, 1954, p. 435.
[18] L. Rayleigh, Philos. Mag. 34 (1892) 481.
[19] M.A. Subramanian, G. Aramudan, G.V. Subba Rao, Prog. Solid State Chem. 15 (1983) 55.
[20] J.F. Ziegler, J.P. Biersack, U. Littmark, The Stopping and Range of Ions in Solids, Pergamon, Oxford, 1985.
[21] M. Perez, Y. Jorba, Ann. Chim. 7 (1962) 479.
[22] C. Ronchi, M. Sheindlin, Int. J. Thermophys. 23 (2002) 293.
[23] N. Chauvin, C. Thiriet-Dodane, J. Noirot, H. Matzke, R.J.M. Konings, T. Wiss, R.P.C. Schram, K. Bakker, E. Neeft, R. Conrad, A. Van Veen, T. Yamashita, EFTTRA Report JRC-ITU-N-2002/39, Institute for Transuranium Elements, Karlsruhe, 2002.
[24] T. Wiss, H. Matzke, V.V. Rondinella, T. Sonoda, W. Assmann, M. Toulemonde, C. Trautmann, Prog. Nucl. Energy 38 (2001) 281.
[25] K.E. Sickafus, H. Matzke, T. Hartmann, K. Yasuda, J.A. Valdez, P. Chodak III, M. Nastasi, R.A. Verrall, J. Nucl. Mater. 274 (1999) 66.
[26] J.L. Lábár, in: L.F. Brno, F. Ciampor (Eds.), EUREM 12, 2000, p. 1379.